



Platinum–titanium alloy catalysts on a Magnéli-phase titanium oxide support for improved durability in Polymer Electrolyte Fuel Cells

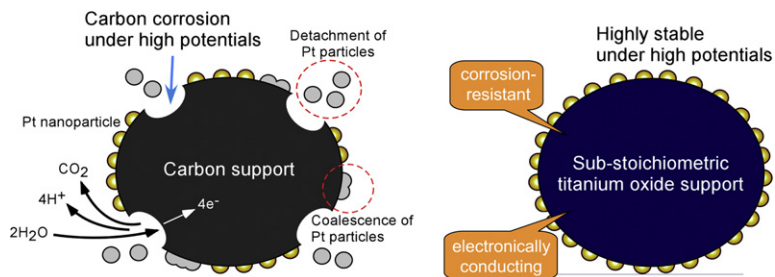
Tsutomu Ioroi*, Tomoki Akita, Masafumi Asahi, Shin-ichi Yamazaki, Zyun Siroma, Naoko Fujiwara, Kazuaki Yasuda

Research Institute for Ubiquitous Energy Devices, National Institute of Advanced Industrial Science and Technology (AIST), 1-8-31 Midorigaoka, Ikeda, Osaka 563-8577, Japan

HIGHLIGHTS

- Corrosion-resistant Pt–Ti alloy/sub-stoichiometric Ti oxide catalysts were prepared.
- Pt–Ti/TiO_x MEA shows a mass activity comparable to that of conventional Pt/XC72.
- Performance loss of Pt–Ti/TiO_x MEA was very limited even after potential cycling to 1.5 V.
- Superior stability of Pt–Ti/TiO_x catalyst under high potential is due to the robustness of the TiO_x support.

GRAPHICAL ABSTRACT



ARTICLE INFO

Article history:

Received 14 September 2012

Accepted 17 September 2012

Available online 23 September 2012

Keywords:

PEFC

Electrocatalyst

Carbon corrosion

Titanium oxide

Magnéli phase

Durability

ABSTRACT

The robustness of the cathode catalysts used in polymer electrolyte fuel cells (PEFCs) is one of the major factors that determines their durability. In this work, a new class of corrosion-resistant catalyst, Pt–Ti alloy nanoparticles deposited on nano-sized sub-stoichiometric titanium oxide (TiO_x), was prepared, and the durability of a Pt–Ti/TiO_x cathode under conditions of fuel cell operation was evaluated. Cell performance under a constant current density for >900 h was examined to demonstrate the practical stability of the Pt–Ti/TiO_x MEA under PEFC operating conditions. To investigate the effect of high potentials on cathode catalyst activity, a potential cycling test between 1.0 V and 1.5 V vs. a hydrogen anode was applied to the MEA. The results indicated that the electrochemical surface area (ECA) of the Pt–Ti/TiO_x MEA is much more stable than that of a conventional Pt/XC72 MEA, and there is almost no loss of ECA even after 10,000 potential cycles. In addition, there was almost no change in the internal resistance of the MEA. TEM analyses of the potential-cycled MEA clearly revealed the excellent stability of Pt nanoparticles supported on TiO_x particles.

© 2012 Elsevier B.V. All rights reserved.

1. Introduction

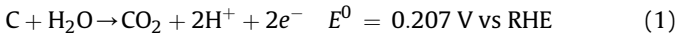
The durability of catalysts in polymer electrolyte fuel cells (PEFCs) is an important issue that must be addressed before their

widespread commercialization in areas such as portable, transportation, and stationary applications, since catalyst durability directly reflects the life and cost of fuel cell power-generation systems [1]. A lifetime of >40,000 h of operation for stationary applications [2] and >5500 h of operation and 10 years in vehicles for automotive applications [3], including load and start/stop cycles, are required. Although many factors could play a role in the mechanism of catalyst degradation, the major contributors are

* Corresponding author. Tel.: +81 72 751 9653; fax: +81 72 751 9629.

E-mail address: ioroi-t@aist.go.jp (T. Ioroi).

believed to be i) dissolution of Pt and re-deposition (Ostwald ripening), ii) coalescence via crystal migration, and iii) detachment of Pt particles from the carbon support [4]. Among these, Pt detachment is strongly affected by corrosion of the carbon support materials [4]. Conventional carbon blacks, such as Vulcan XC72, are superior catalyst-support materials because of their cost and physicochemical properties. However, carbon is not stable based on thermodynamic considerations under the cathode conditions in a PEFC:



Although this reaction proceeds slowly at potentials <0.8 V in a PEFC [5], corrosion reactions are significantly accelerated under high potential conditions, such as with the cathode at OCV (~ 1.0 V), potential excursions due to a H_2 /air front and local H_2 starvation (~ 1.5 V) [6–8], which may lead to a significant loss of cell performance [9]. Therefore, alternative catalyst-support materials that are highly oxidation-resistant are necessary. To improve the stability of the catalyst support, considerable work has been done over the past few decades on non-carbon support materials, including oxides, carbides, and nitrides [10–12]. Among these, we have focused on oxygen-deficient, sub-stoichiometric titanium oxide (Ti_nO_{2n-1} , known as Magnéli phase), and in particular Ti_4O_7 , and have demonstrated the potential of Ti_4O_7 -supported Pt for use as an oxidation-resistant cathode catalyst in PEFCs [13,14]. In addition, Magnéli-phase oxides (TiOx) with a high specific surface area have been also prepared by a UV laser irradiation technique [15]. This leads to improved specific activity for the oxygen reduction reaction (ORR) due to the formation of Pt–Ti alloy particles on the TiOx support, as well as the improved dispersion of Pt due to the deposition of smaller catalyst particles [16].

The purpose of this study was to evaluate the activity and stability of Pt–Ti/TiOx cathodes under PEFC operating conditions, and especially at high potential conditions. The basic performance of Pt–Ti/TiOx cathode catalysts under the initial conditions and after >900 h of operation is reported. The oxidation-resistant properties of Pt–Ti/TiOx catalysts were also examined by using an

accelerated stress test protocol, and compared to those of a conventional Pt/XC72 catalyst.

2. Experimental

2.1. Preparation of TiOx-supported platinum catalysts

Pt–Ti/TiOx catalysts with a platinum loading of 10–20 wt% were prepared by an impregnation-reduction process, using nano-submicron TiOx particles as a support. A TiOx support was prepared by the irradiation of TiO_2 nanoparticles with a Nd:YAG pulsed laser, as described previously [15]. Briefly, a fine TiO_2 powder (Ishihara Sangyo Kaisha, >99.99%, 70 nm typical diameter, PT-401M) was dispersed in acetonitrile and irradiated for 1 h with a pulsed UV laser (Continuum, SureliteIII) at a wavelength of 355 nm. The laser-irradiated TiOx dispersion was filtered and washed with 0.5 M H_2SO_4 solution at 50–70 °C for 2 h to remove impurities, and then used as a catalyst-support material. The details of Pt deposition on TiOx have also been described previously [16]. Briefly, 1 g of laser-irradiated TiOx powder was dispersed in an ethanol solution of $Pt(NO_2)_2(NH_3)_2$ (Ishifuku Metal Industry), and the mixture was vigorously stirred and dried at ca. 70 °C. The resulting mixture precursor was then heated at 900 °C for 1 h under a continuous flow of H_2 at a rate of 100 mL min⁻¹ and allowed to cool to room temperature. To remove impurities and contamination of the catalyst, the prepared Pt–Ti/TiOx catalyst was re-dispersed in 0.5 M H_2SO_4 solution at 80 °C and stirred for 2 h. After being filtered, washed with DI water and dried in an oven at 100 °C for at least 3 h, the prepared Pt–Ti/TiOx catalysts were used for the following physicochemical and electrochemical analyses. For comparison, a conventional carbon-supported platinum catalyst supplied by Tanaka Kikinzoku Kougyo (TEC10V40E; 37.9 wt% Pt on Vulcan XC72) was used as a reference (hereafter referred to as Pt/XC72).

The crystal structure of the obtained Pt–Ti/TiOx particles was checked by X-ray diffraction (XRD) measurements using a Rigaku RINT-Ultima⁺ with a Cu K α X-ray source. The morphology of the catalysts was observed with a JEOL JSM-6400F scanning electron

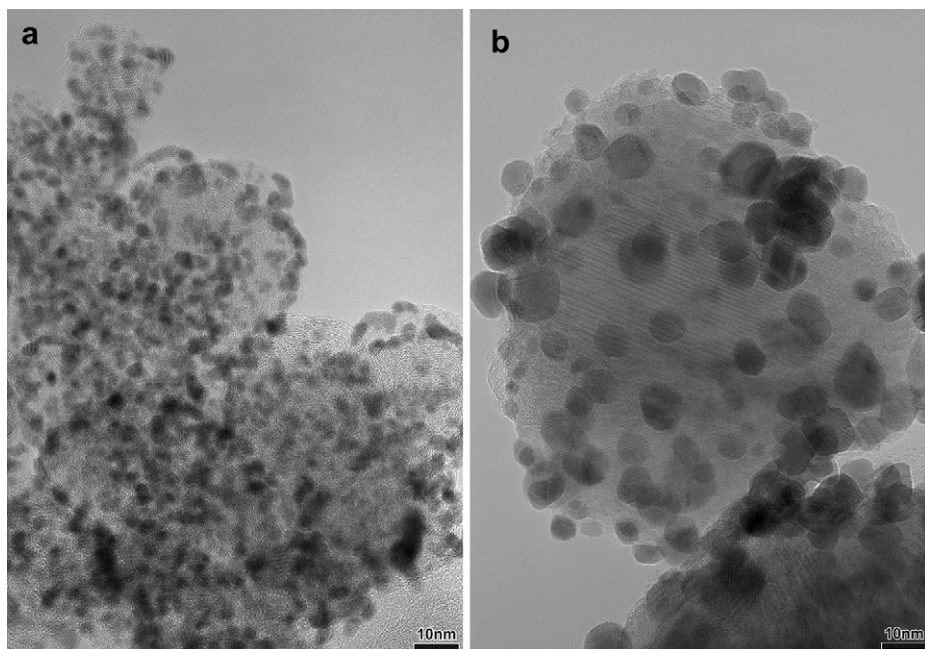


Fig. 1. TEM images of (a) 40 wt% Pt/XC72 and (b) 10 wt% Pt–Ti/TiOx.

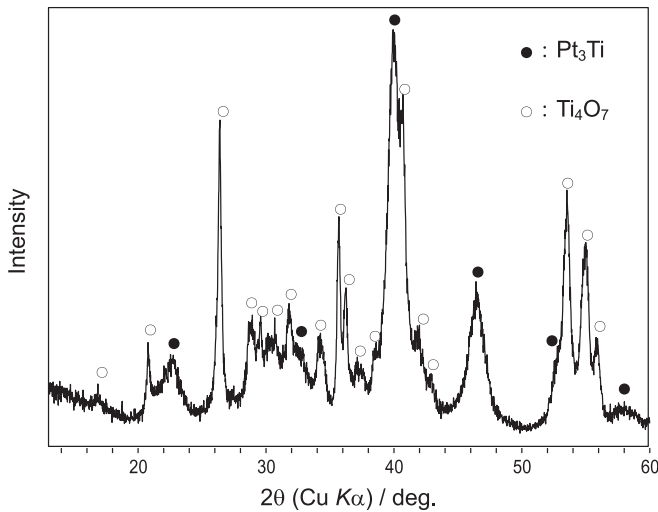


Fig. 2. XRD pattern of 10 wt% Pt–Ti/TiOx.

microscope (SEM). The atomic structure of Pt–Ti/TiOx was observed by a JEOL JEM-3000F transmission electron microscope (TEM).

2.2. MEA fabrication and performance/durability testing

All of the electrochemical properties of the catalysts were examined by testing using a small-scale single cell (active area of 25 cm²). Membrane electrode assemblies (MEAs) used in this work were prepared with the Pt–Ti/TiOx and Pt/XC72 catalysts for the cathode and the Pt/XC72 catalyst for the anode. For each electrocatalyst layer of the MEA, the platinum loading was 0.5 mg cm⁻². Pretreated DuPont Nafion 112 or NRE-212 (50 μm thick) was used as an electrolyte membrane and SGL SIGRACET GDL35BC (350 μm thick, including a microporous layer), and/or GDL35BA (without a microporous layer) were used as gas diffusion layers. MEA was fabricated by the modified “decal method” [17]. A catalyst ink

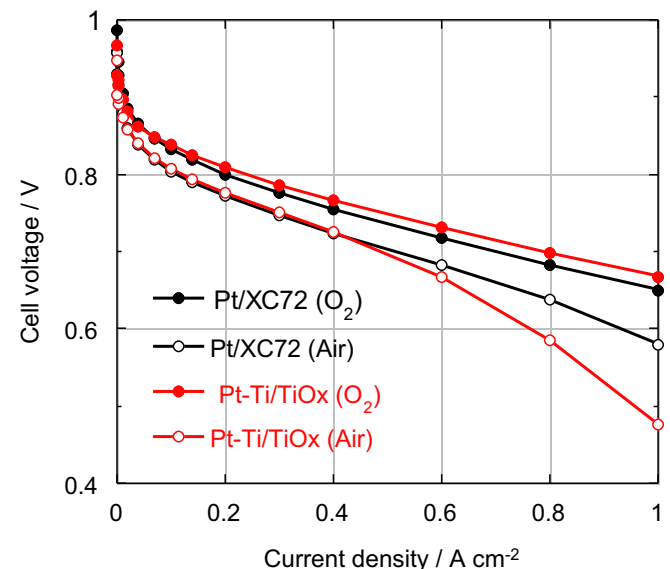


Fig. 4. Initial H₂/O₂ and H₂/air performance curves of MEAs with 20 wt% Pt–Ti/TiOx and 40 wt% Pt/XC72 catalysts on the cathode at 80 °C. The flow rates of H₂, O₂ and air were 272, 136, and 1131 cm³ min⁻¹, respectively.

mixture of 0.35 g Nafion solution (Aldrich, 5 wt% solution), 0.35 g Pt–Ti/TiOx catalyst and 0.14 g 2-propanol was coated on polytetrafluoroethylene (PTFE) film (50 μm thick), and dried in a vacuum oven at 80 °C. A catalyst layer of Pt/XC72 was prepared in a similar manner, using 0.2 g Pt/XC72 and 1.2 g Nafion solution. These electrocatalyst layers were hot-pressed at 140 °C for 2 min on both sides of a Nafion membrane. An MEA was sandwiched between two gas diffusion layers to form a single cell testing unit. Cell operating conditions were 80 °C at ambient pressure with a supply of hydrogen and oxygen (air) humidified at 80 °C for H₂ and 77 °C for O₂ as reactants.

To evaluate the initial performance of the MEA, polarization measurements and cyclic voltammetry (CV) were conducted. During polarization curve measurements, the cell voltage was controlled by an electronic load (Kikusui, PLZ164WA). The cell was held at each current density for 5 min before the voltages were recorded and the polarization curves were taken from a high to low

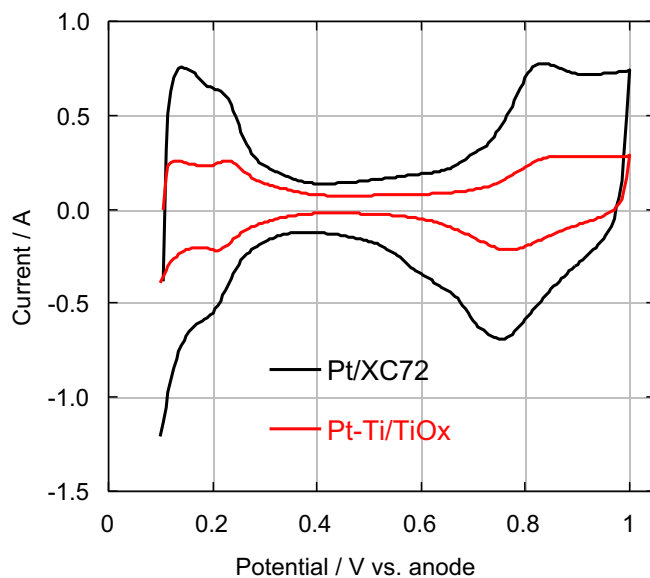


Fig. 3. Cyclic voltammograms of MEAs with 20 wt% Pt–Ti/TiOx and 40 wt% Pt/XC72 cathodes bonded to an N112 membrane. Electrode geometric area: 25 cm², Pt loading: 0.5 mg-Pt cm⁻². Cell temperature: 80 °C, ambient pressure, scan rate 100 mV s⁻¹.

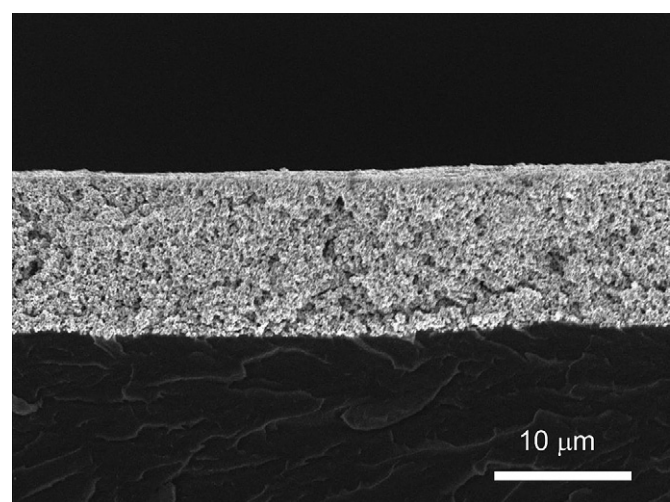


Fig. 5. A typical SEM image of a cross-section of a 20 wt% Pt–Ti/TiOx cathode/membrane interface at the initial state.

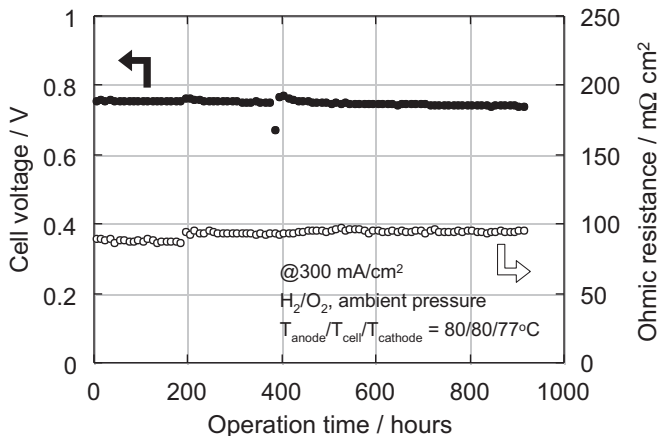


Fig. 6. Pt–Ti/TiOx MEA performance test under constant current mode; electrode geometric area: 25 cm², H₂/O₂ flow rate: 82/100 cm³ min⁻¹, anode: 40 wt% Pt/XC72 (0.42 mg-Pt cm⁻²)/SGL35BA, cathode: 20 wt% Pt–Ti/TiOx (0.43 mg-Pt cm⁻²)/SGL35BC, NRE-212 membrane.

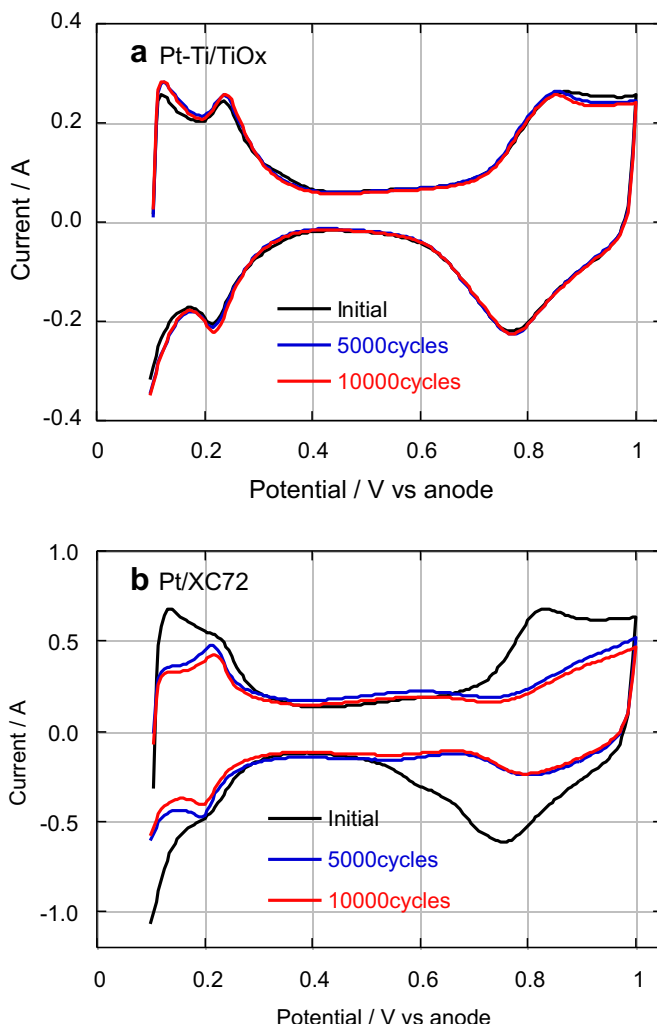


Fig. 7. Cyclic voltammograms of MEAs with (a) 20 wt% Pt–Ti/TiOx and (b) 40 wt% Pt/XC72 cathodes operated at 80 °C under N₂ flow conditions at the initial state, and after 5000/10,000 cycles of potential sweeps. Potential sweep: 1.0–1.5 V vs. anode, 500 mV s⁻¹.

current density. The flow rates of hydrogen, oxygen and air were fixed at 272, 136 and 1131 cm³ min⁻¹, respectively, which correspond to a stoichiometry of 1.43, 1.43 and 2.5, respectively at 25 A. During CV measurements, fully humidified hydrogen and nitrogen were fed to the anode and cathode, and voltammograms were recorded between 0.05 and 1.0 V at a scan rate of 100 mV s⁻¹ by using a potentiostat/galvanostat (ALS, Model 660) with a current booster (ALS, Model 680). All potentials in this paper are referred to the anode because anode polarization is negligibly small during CV measurements (quasi-reference electrode).

To examine the stability of the catalysts under high potential conditions, which are expected to arise during start/stop periods, the effects of high potentials at >1.0 V on the catalysts were evaluated by the stability testing protocols recommended by the Fuel Cell Commercialization Conference of Japan (FCCJ) [18]; repeated potential cycling of the cathode between 1.0 and 1.5 V at 500 mV s⁻¹, cell temperature: 80 °C. During testing, fully humidified hydrogen and nitrogen were fed to the anode and cathode. For cell diagnosis, the electrochemically active area (ECA) of the catalyst was periodically evaluated by CVs after 500, 1000, 2000, 5000, 7500 and 10,000 potential cycles.

To characterize the changes in the catalyst after stability testing, TEM observations of the catalyst particles and XRD measurements of catalyst layers were conducted for the MEAs.

3. Results and discussion

3.1. Pt–Ti/TiOx catalyst characterization and initial catalyst activity

The morphology of Pt–Ti/TiOx catalyst particles and the crystal structures of Pt and TiOx were characterized by TEM and XRD, as shown in Figs. 1 and 2. As discussed previously [16], the uniform deposition of Pt particles was observed, however, Pt particles in Pt–Ti/TiOx were larger than the Pt in Pt/XC72 catalyst. This is primarily due to the low specific surface area of TiOx compared to XC72 and the high temperature used during catalyst preparation. In the XRD pattern, almost all of diffraction peaks are assigned to Magnéli-phase Ti₄O₇ (Ti_nO_{2n-1}/n = 4) and ordered Pt₃Ti. Notably, no higher order Magnéli phase such as Ti₅O₉ (n = 5)

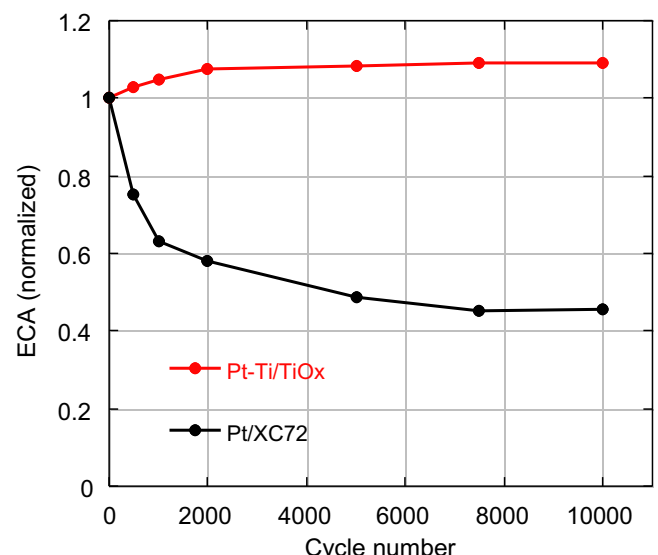


Fig. 8. Plots of the normalized electrochemically active area (ECA) of MEAs with 20 wt% Pt–Ti/TiOx and 40 wt% Pt/XC72 cathodes as a function of the number of potential cycles. For the experimental conditions, see Fig. 7.

was detected. This is important for practical catalyst applications because higher oxides are less conductive, which would lead to a greater ohmic loss in the catalyst layer.

The electrochemical activity and stability of Pt–Ti/TiO_x as a cathode catalyst were evaluated by using MEAs operated at 80 °C, under a fully humidified condition. Fig. 3 shows CVs of Pt–Ti/TiO_x and Pt/XC72 catalysts. As expected from the results of TEM (Fig. 1), the ECA of Pt–Ti/TiO_x is less than that of Pt/XC72. The coulombic charge of the hydrogen UPD peak of Pt–Ti/TiO_x is ca. 38% of that of Pt/XC72, which is consistent with the value determined by RDE (36%) [16]. This fact indicates that Pt–Ti/TiO_x particles in MEA are sufficiently covered with ionomer to give an adequate electrochemical response. Fig. 4 shows the H₂/O₂ and H₂/air polarization curves of MEAs using Pt–Ti/TiO_x and Pt/XC72 catalysts. In H₂/O₂ performance, the Pt–Ti/TiO_x MEA shows a voltage comparable to or slightly higher than that of Pt/XC72. For Pt–Ti alloy catalysts, an enhancement of kinetic activity for ORR has been reported in the literature [19,20]. Ding reported that the enhancement of activity of

carbon-supported Pt–Ti alloy catalysts for ORR was affected by the titanium concentration, and Pt₇₅Ti₂₅ shows the maximum activity, with an enhancement factor of 1.8–1.9 [19]. Therefore, the smaller ECA of Pt–Ti/TiO_x is counteracted by this activity-enhancement to give similar performance in this case. In contrast, Pt–Ti/TiO_x shows different behavior in the H₂/air condition; Pt–Ti/TiO_x showed a lower voltage than Pt/XC72 at a current density of >0.4 A cm⁻², which indicated a greater mass transport loss for the Pt–Ti/TiO_x MEA. To confirm the structure of the catalyst layer, a fractured cross-section of the pristine MEA was observed. Fig. 5 shows a cross-sectional view of MEA at the interface between the Pt–Ti/TiO_x catalyst layer and the Nafion membrane. The catalyst layer was ca. 10 μm thick, which is almost the same as the thickness of the Pt/XC72 cathode with the same amount of Pt loading. However, the calculated pore volume ratio of the Pt–Ti/TiO_x layer is only ca. 44%, which is less than that of the Pt/XC72 layer (58%). This may be due to the difference in the microstructure of the catalyst layer. In conventional Pt/XC72, carbon particles are connected to each other to form a micronetwork structure, which leads to a porous catalyst layer. On the other hand, there is less interconnection of TiO_x particles [15], so that the Pt–Ti/TiO_x catalyst layer tends to be more dense.

To examine the long-term catalyst stability under constant current load conditions, the Pt–Ti/TiO_x MEA was operated for >900 h. The measured trends of cell voltage and ohmic resistance are shown in Fig. 6 (operating conditions are shown in the figure). The cell voltage and ohmic resistance of Pt–Ti/TiO_x MEA were fairly stable under the actual PEFC operating condition within the time range of this test. This indicates that Pt–Ti/TiO_x have sufficient potential for practical application as a PEFC cathode catalyst material.

3.2. Pt–Ti/TiO_x catalyst stability at high potentials

Recently, it has been demonstrated that corrosion of the catalyst-support materials in a PEFC is accelerated during start/shutdown periods, which is due to an abnormally high potential arising at the cathode, which is caused by a non-uniform gas distribution in the anode gas channel, as reported in the literature [6]. To simulate and accelerate such high potential conditions,

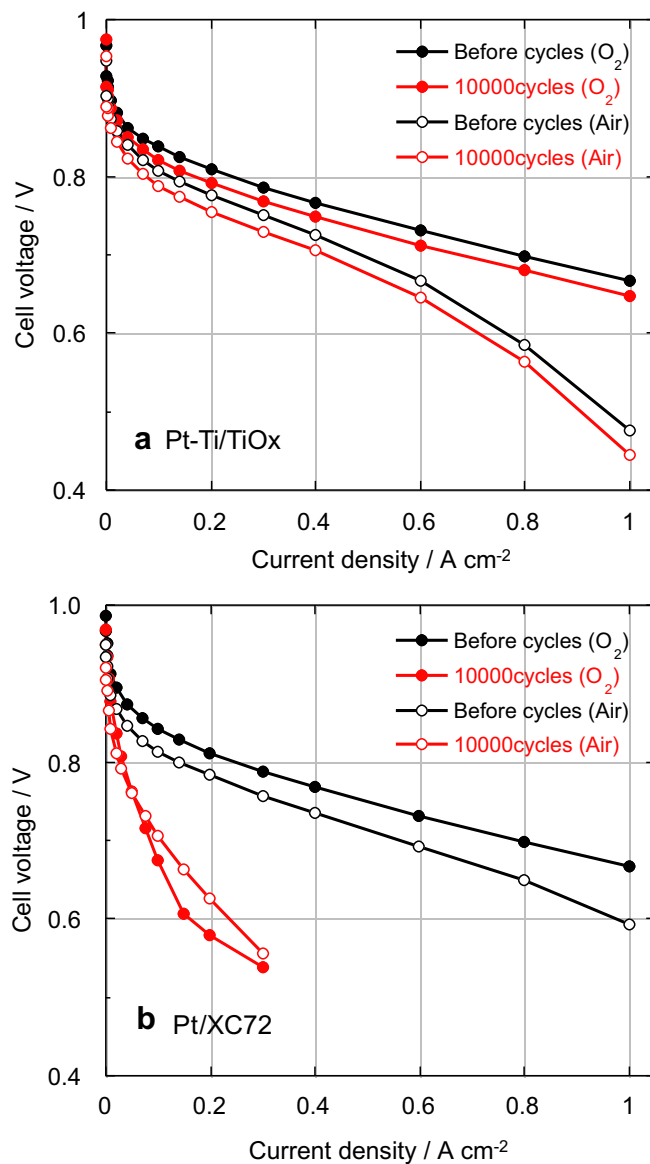


Fig. 9. H₂/O₂ and H₂/air performance curves of MEAs with (a) 20 wt% Pt–Ti/TiO_x and (b) 40 wt% Pt/XC72 catalysts on the cathode at 80 °C before and after potential cycling. The flow rates of H₂, O₂ and air were 272, 136, and 1131 cm³ min⁻¹, respectively.

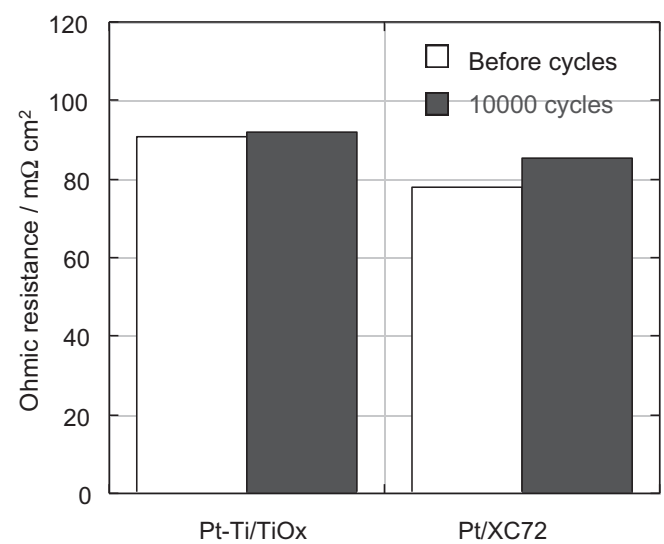


Fig. 10. Ohmic resistance of 20 wt% Pt–Ti/TiO_x and 40 wt% Pt/XC72 MEAs before and after potential cycling. Operating conditions: cell temp.: 80 °C, H₂/O₂ feed, 300 mA cm⁻² load.

a repeated potential cycling test was conducted by subjecting the cathode to a potential sweep of 1.0 and 1.5 V vs. the anode at a sweep rate of 500 mV s⁻¹ [18]. For cell diagnosis, the electrochemically active area (ECA) of the catalyst was evaluated by the use of CVs after 500, 1000, 2000, 5000, 7500 and 10,000 potential cycles. Cell performance was also evaluated after 2000 and 10,000 cycles. This test was started after >100 h of operation of MEA with fully humidified H₂/O₂ at 80 °C (@300 mA cm⁻²) to avoid the initial instability of performance in the break-in period. Fig. 7 shows typical CVs of Pt–Ti/TiO_x and Pt/XC72 MEA cathodes at the initial state and after 5000 and 10,000 cycles of potential sweeps. CVs of Pt–Ti/TiO_x MEA were essentially unchanged even after 10,000 cycles, which is consistent with the previous RDE results [16]. In contrast, the rapid shrinkage of Pt redox peaks and an increase in the double layer charging current were observed for CVs of Pt/XC72 MEA, which indicated a loss of ECA mainly due to corrosion of the carbon support. The ECAs during the potential cycle test were calculated for CVs in Fig. 7, by assuming that the coulombic charge

of the monolayer of H_{UPD} adsorbed on Pt is 210 μC cm⁻²-Pt. Fig. 8 shows the normalized ECA of the MEAs as a function of the cycle number of the potential sweep between 1.0 and 1.5 V. As shown in Fig. 8, the Pt/XC72 MEA lost ca. 40% ECA within the first 1000 cycles, and the rate of ECA loss slowed thereafter. Siroma investigated the electrochemical corrosion of carbon materials at high potentials in 1 M H₂SO₄ solution, and found that a relatively high rate of corrosion was observed at the beginning of the test [21]. This result indicates that some of the carbon surface is more vulnerable to corrosion at high potential. Thus, the rapid loss of ECA for Pt/XC72 in Fig. 8 may also be ascribed to rapid carbon corrosion. In contrast, the ECA of Pt–Ti/TiO_x MEA is very stable due to the high stability of the TiO_x support at high potentials. The cell performance and ohmic resistance of the Pt–Ti/TiO_x and Pt/XC72 MEAs before and after potential cycling are shown in Figs. 9 and 10, respectively. Although a slight voltage loss was observed after potential cycling, the Pt–Ti/TiO_x MEA shows relatively stable performance with both H₂/O₂ and H₂/air, compared to the Pt/XC72 MEA, which showed

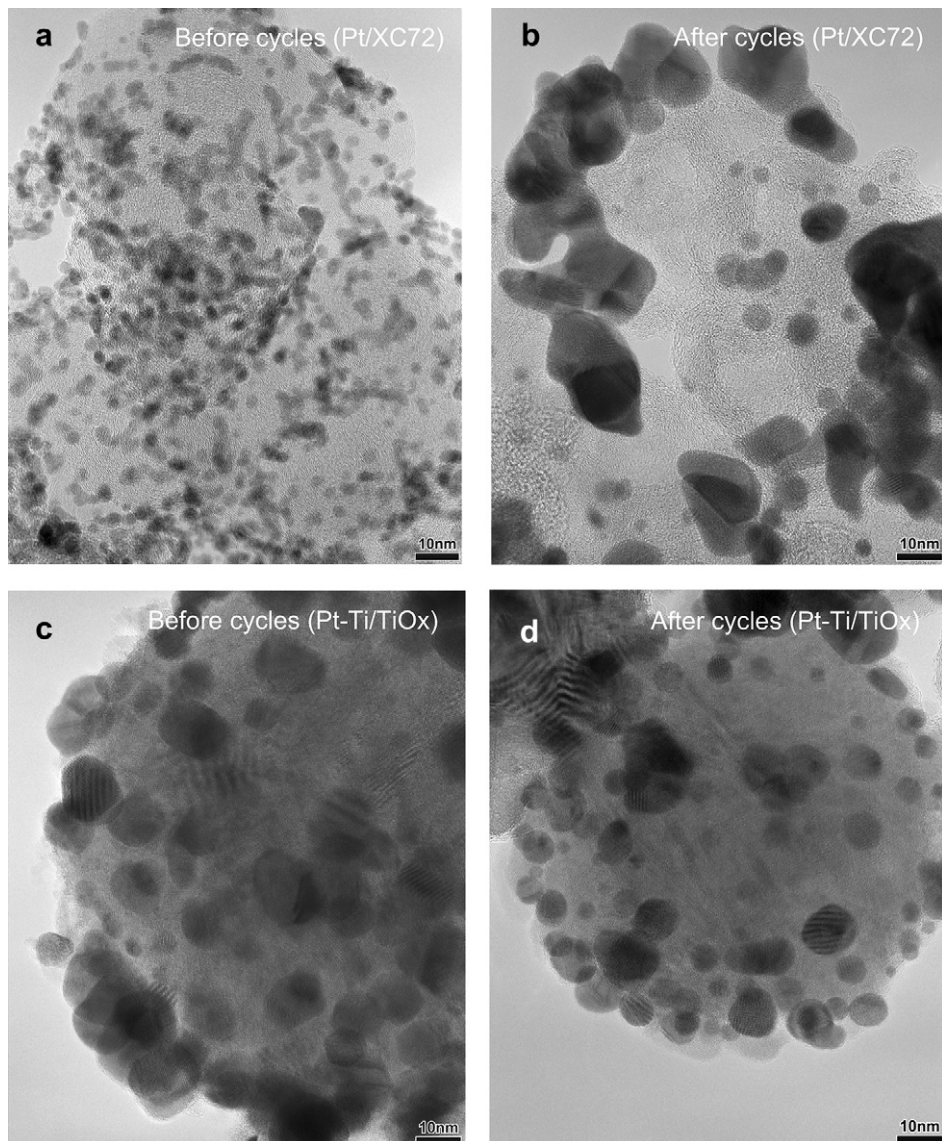


Fig. 11. TEM images of MEA cathodes with (a) 40 wt% Pt/XC72 before potential cycling, (b) 40 wt% Pt/XC72 after 1000 potential cycles, (c) 20 wt% Pt–Ti/TiO_x before potential cycling, and (d) 20 wt% Pt–Ti/TiO_x after 1000 potential cycles. Operating conditions: cell temp.: 80 °C, ambient pressure. Potential cycling conditions: 0.9/1.3 V vs. anode, rectangular wave, hold at each potential: 30 s.

considerable performance degradation. Since potential cycling did not cause a loss of ECA for Pt–Ti/TiO_x, as described above, and the increase in ohmic resistance of Pt–Ti/TiO_x MEA was also very limited, as shown in Fig. 10, it is plausible that this slight voltage loss of Pt–Ti/TiO_x MEA may be ascribed to a loss of the specific activity of the Pt–Ti catalyst. In Pt-3d metal alloy catalysts, it is thought that a loss of specific activity over time during fuel cell operation or voltage cycling results from the dissolution of platinum and transition metal. Carlton observed Pt₃Co nanoparticles after potential cycling (0.65/1.05 V vs. RHE at 80 °C) by using sub-nanometer-resolution TEM, and found that the Pt-enriched-shell became thicker after voltage cycling [22]. A similar dissolution of Ti during potential cycling is also expected in the Pt–Ti system, which may affect MEA performance.

To examine the influence of potential cycling on the structure of the Pt–Ti/TiO_x catalyst, the tested MEA was analyzed by a scanning TEM (STEM) equipped with EDX. Several locations at the center and perimeter of the Pt–Ti nanoparticles were selected and the Pt/Ti atomic composition at each location was determined by using a narrowed electron beam (beam diameter <1 nm). Although more than 10 points were examined, we did not find a significant difference between the pristine and potential-cycled catalysts within the accuracy of the instruments. This indicates that Ti dissolution may be limited to the very surface (<1 nm) of the Pt–Ti particles under the present experimental conditions. This is consistent with the XRD pattern of the tested Pt–Ti/TiO_x MEA, where no peak-shift was observed for the Pt–Ti diffraction patterns (not shown). Fig. 11 shows TEM images of the catalyst particles of Pt–Ti/TiO_x and Pt/XC72 MEAs before and after 1000 potential cycling (0.9/1.3 V, rectangular wave, hold at each potential: 30 s; former FCCJ protocol [23]). The intensive growth of Pt particles was observed for Pt/XC72, which is consistent with the literature [4,24]. Three main paths have been proposed for the degradation mechanism of Pt/C catalysts: Pt dissolution and re-deposition (growth via Ostwald ripening), coalescence via crystal migration, and detachment of Pt particles from the carbon support [4]. Interestingly, the Pt particles found in cycled Pt/XC72 MEA have a very irregular shape. In contrast, only the coarsening of spherically-shaped Pt particles was observed under lower upper-limit potential cycling (~1.0 V vs. RHE) [25]. This difference may be due to the more intensive carbon corrosion under higher voltages, since carbon corrosion promotes particle coalescence via crystal migration, which likely leads to the formation of such irregularly-shaped Pt particles. On the other hand, Pt particles of Pt–Ti/TiO_x MEA were almost unchanged. Strong interaction between Pt particles and the oxide support with superior stability against high potentials could account for this structural stability of Pt–Ti/TiO_x.

4. Conclusions

The cell performance and durability of a Pt–Ti/TiO_x MEA under actual operating condition were demonstrated, and compared to those of a conventional carbon-supported catalyst. The Pt–Ti/TiO_x MEA could be operated stably for >900 h and showed a mass

activity comparable to that of Pt/XC72 MEA. A potential cycling test up to 1.5 V vs. RHE was conducted to examine the durability of the catalysts against high potentials. The results indicate that the Pt–Ti/TiO_x MEA exhibits greater stability for both the ECA and cell performance. A post-cycling analysis of the tested MEA clearly revealed that the high stability of Pt–Ti/TiO_x is due to the robustness of the TiO_x support.

Acknowledgments

This work was supported in part by the “Strategic Development of PEFC Technologies for Practical Application” project of New Energy and Industrial Technology Development Organization (NEDO), Japan.

References

- [1] R. Borup, J. Meyers, B. Pivovar, Y.S. Kim, R. Mukundan, N. Garland, D. Myers, M. Wilson, F. Garzon, D. Wood, P. Zelenay, K. More, K. Stroh, T. Zawodzinski, J. Boncella, J.E. McGrath, M. Inaba, K. Miyatake, M. Hori, K. Ota, Z. Ogumi, S. Miyata, A. Nishikata, Z. Siroma, Y. Uchimoto, K. Yasuda, K. Kimijima, N. Iwashita, *Chem. Rev.* 107 (2007) 3904–3951.
- [2] S. Cleghorn, D. Mayfield, D. Moore, G. Rusch, T. Sherman, N. Sisofo, U. Beuscher, *J. Power Sources* 158 (2006) 446–454.
- [3] M. Mathias, R. Makharia, H. Gasteiger, J. Conley, T. Fuller, C. Gittleman, S. Kocha, D. Miller, C. Mittelstaedt, T. Xie, S. Yan, P. Yu, *Interface (USA)* 14 (2005) 24–35.
- [4] Y. Shao-Horn, W. Sheng, S. Chen, P. Ferreira, E. Holby, D. Morgan, *Top. Catal.* 46 (2007) 285–305.
- [5] R. Makharia, S. Kocha, P. Yu, M. Sweikart, W. Gu, F. Wagner, H. Gasteiger, *ECS Trans.* 1 (8) (2006) 3–18.
- [6] C. Reiser, L. Bregoli, T. Patterson, J. Yi, J. Yang, M. Perry, T. Jarvi, *Electrochem. Solid-State Lett.* 8 (2005) A273–A276.
- [7] T. Patterson, R. Darling, *Electrochem. Solid-State Lett.* 9 (2006) A183–A185.
- [8] A. Taniguchi, T. Akita, K. Yasuda, Y. Miyazaki, *J. Power Sources* 130 (2004) 42–49.
- [9] P. Yu, W. Gu, R. Makharia, F. Wagner, H. Gasteiger, *ECS Trans.* 3 (1) (2006) 797–809.
- [10] E. Antolini, E. Gonzalez, *Solid State Ionics* 180 (2009) 746–763.
- [11] Y. Shao, J. Liu, Y. Wong, Y. Lin, *J. Mater. Chem.* 19 (2009) 46–59.
- [12] Y. Wang, D. Wilkinson, J. Zhang, *Chem. Rev.* 111 (2011) 7625–7651.
- [13] T. Ioroi, Z. Siroma, N. Fujiwara, S. Yamazaki, K. Yasuda, *Electrochem. Commun.* 7 (2005) 183–188.
- [14] T. Ioroi, H. Senoh, S. Yamazaki, Z. Siroma, N. Fujiwara, K. Yasuda, *J. Electrochem. Soc.* 155 (2008) B321–B326.
- [15] T. Ioroi, H. Kageyama, T. Akita, K. Yasuda, *Phys. Chem. Chem. Phys.* 12 (2010) 7529–7535.
- [16] T. Ioroi, T. Akita, S. Yamazaki, Z. Siroma, N. Fujiwara, K. Yasuda, *J. Electrochem. Soc.* 158 (2011) C329–C334.
- [17] M. Wilson, S. Gottesfeld, *J. Appl. Electrochem.* 22 (1992) 1–7.
- [18] A. Ohma, K. Shinohara, A. Iiyama, T. Yoshida, A. Daimaru, *ECS Trans.* 41 (2011) 775–784.
- [19] E. Ding, K. More, T. He, *J. Power Sources* 175 (2008) 794–799.
- [20] V.R. Stamenkovic, B.S. Mun, M. Arenz, K.J. Mayrhofer, C.A. Lucas, G. Wang, P.N. Ross, N.M. Markovic, *Nat. Mat.* 6 (2007) 241–247.
- [21] Z. Siroma, M. Tanaka, K. Yasuda, K. Tanimoto, M. Inaba, A. Tasaka, *Electrochemistry* 75 (2007) 258–260.
- [22] C. Carlton, S. Chen, P. Ferreira, L. Allard, Y. Shao-Horn, *J. Phys. Chem. Lett.* 3 (2012) 161–166.
- [23] http://fccj.jp/pdf/19_01_kt.pdf (in Japanese).
- [24] K. Yasuda, A. Taniguchi, T. Akita, T. Ioroi, Z. Siroma, *Phys. Chem. Chem. Phys.* 8 (2006) 746–752.
- [25] P. Ferreira, G. la O', Y. Shao-Horn, D. Morgan, R. Makharia, S. Kocha, H. Gasteiger, *J. Electrochem. Soc.* 152 (2005) A2256–A2271.